2022

Numerical Investigation on Effects of Sub-cooled & Super-heating degree on Performance of VRF System with Simultaneous Operation

Been Oh

Dongwon Kim

Hosik Jeong

Yeseul Park

Jiyeon Choi

See next page for additional authors

Numerical Investigation on Effects of Sub-cooled & Super-heating Degree on Performance of VRF System with Simultaneous Operation

Been Oh[1], Dongwon Kim[1], Hosik Jeong[1], Yeseul Park[1], Jiyeon Choi[3], Byungchae Min[3], Gyunmin Choi[2]*

[1]School of Mechanical Engineering, Pusan National University,
Busan, Korea
(obeen93@pusan.ac.kr, kimdw@pusan.ac.kr, wjdghtlr18@pusan.ac.kr, ysparkk@pusan.ac.kr)

[2]Department of Mechanical Engineering, Pusan National University,
Busan, Korea
(choigm@pusan.ac.kr)

[3]SAC Research/Engineering Division, H&A Solution company, LG Electronics,
Changwon, Korea
(jiyeon26.choi@lge.com, byungchae.min@lge.com)

ABSTRACT

Recently, the simultaneous cooling and heating operation is applied to the heat pump system. The simultaneous operation is one of the prospective functions for the VRF system. Since there are few studies on the simultaneous operation of the VRF system, detail studies are needed to increase the efficiency of simultaneous operation. Numerical analysis was conducted to investigate the performance and its energy saving potential of the VRF system with simultaneous cooling and heating operation. And the simulation results were validated with the experimental ones. The VRF system was controlled by the set subcooling or superheating degree of indoor unit and outdoor unit. The energy consumption of the VRF system was affected by compressor rpm, fan speed, set point temperature and ambient temperature. And the performance of the VRF system was varied from the number of operating indoor units and the thermal load of indoor unit. The optimal point was observed according to the heat balance of indoor unit. In this system. Additionally, the performance of the VRF system was studied the effect of parameters for each thermal load of indoor unit.

1. INTRODUCTION

The VRF systems have been used in residential buildings as HVAC units under hot season and cold season because of its high efficiency, saving installation space and convenient individual control in separated zones. The VRF system is a multi-segment air conditioning system that can independently vary the flow rate of refrigerant flowing into the indoor unit of each zone and can be adjusted according to various and dynamic space cooling or heating loads. A variety of advanced control technologies including variable rotational fan speed, variable displacement compressors with inverter technology. As for the VRF system, a system capable of cooling and heating at the same time in each indoor unit connected to one outdoor unit is becoming widespread. The reason for the increase in the supply of simultaneous heating and cooling products is that if there are offices that require heating in winter and computer rooms that require cooling in the air conditioning space of a building, heating and cooling operation can be performed according to each air conditioning condition, thereby satisfying the various needs of consumers. there is. In addition, the simultaneous heating and cooling heat pump system is a high-efficiency system that can increase thermal efficiency by more than 30% because it is operated by recovering waste heat unlike general heat pump systems.
Researchers have been studying the simultaneous operation of cooling and heating operation of VRF system. Zhang et al (2018) proposed a new control algorithm using a physical model according to the load on the indoor unit. An optimization algorithm for each operation was developed using energy plus by subdividing the operation mode of the system according to the ratio of cooling capacity and heating capacity. Hong et al (2017) develop a new model of the VRF system to simulate the energy performance. They are described the algorithm of the new model and They implemented the model through Energy Plus and verified the model through field tests. Most researchers conduct

Table 1: Specifications of the components

Components	Type	Specifications
Compressor	Scroll type	Displacement volume : 61.1cm^3/rev Rotational speed : Max. 120Hz
Indoor unit heat exchanger	Finned tube type	Fin type : Louver fin L 1.8 x W 1
Outdoor unit heat exchanger	Plate type	L 0.47 x W 0.119

research on simultaneous operation of VRF systems through algorithms or field tests. In the VRF system with simultaneous operation (cooling and heating), it is necessary to analyze the effect of each parameter on the system. In this study, the performance change according to the degree of superheating or subcooling of the indoor unit and the combination in the simultaneous operation of cooling and heating was studied through numerical analysis in a water-cooled VRF system.

2. EXPERIMENTAL APPARATUS

This study was conducted in a water-cooled VRF system. According to the load of the indoor unit, it can be divided into a cooling-based mode and heating-based mode. If the cooling load of indoor units is larger than that of heating, the cooling-based mode is used. Conversely, if the heating load is larger, it operates in the heating-based mode. The performance of the VRF system was evaluated according to AHRI Standard 1230. The outdoor unit is connected to 12 indoor units. And the outdoor unit consists of compressor, two four-way valves, a plate type heat exchanger, an oil separator, and an accumulator. The indoor units consist of an EEV and a louver fin type heat exchanger. The specifications of the components are shown in table 1. The Schematic diagram of experimental apparatus is shown in Fig 1. The refrigerant flow path is different in the cooling-based mode and in the heating-based mode.

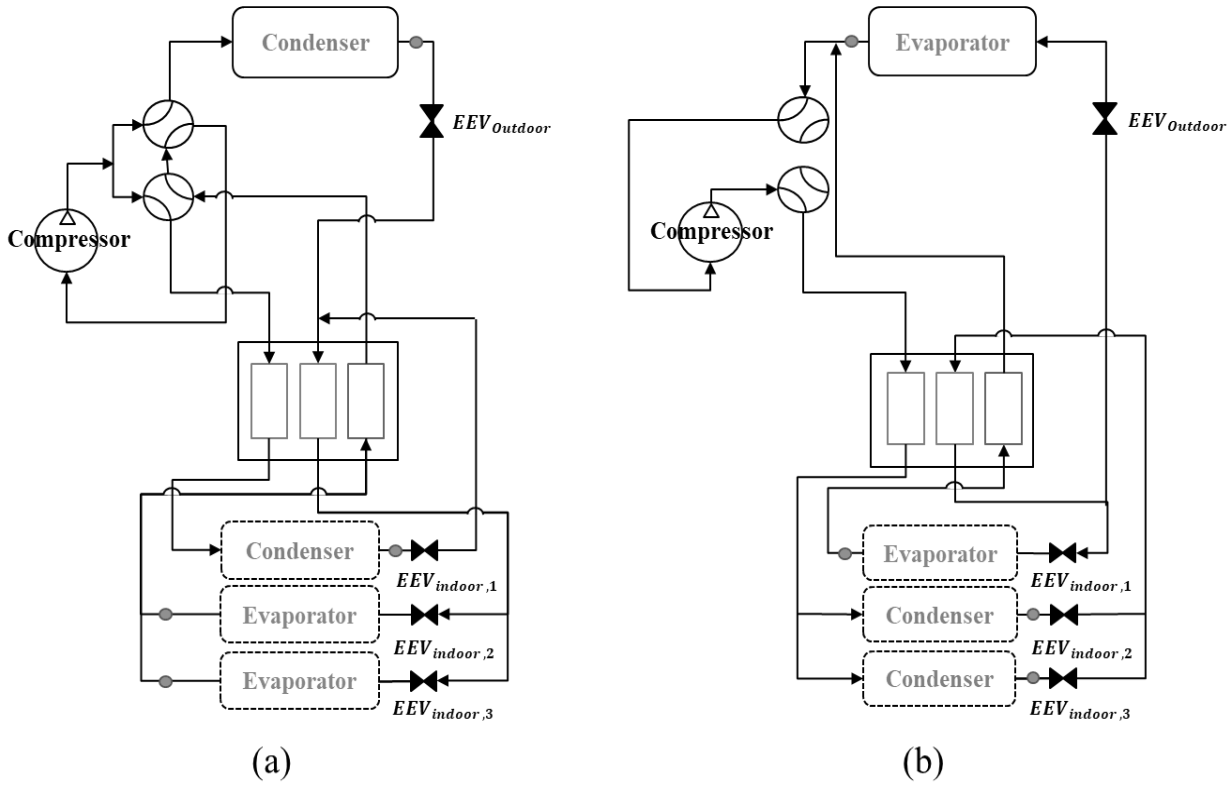

Figure 1: Schematic diagram of VRF system (a) Cooling based mode (b) Heating based mode

3. MATHMATICAL MODELS

3.1 Scroll Compressor

The scroll compressor was calculated with geometry-based model proposed by Kwon et al. This model calculated the energy consumption and the mass flow rate of the scroll compressor. The thermodynamic model satisfies the law of conservation of mass and the law of conservation of energy in the process of suction, compression, and discharge. The law of conservation of mass and energy were expressed in Eq. (1), (2) respectively.

$$\frac{dm}{d\theta} = \frac{dm_{in}}{d\theta} - \frac{dm_{out}}{d\theta} \tag{1}$$

$$M\frac{dh}{dt} = \dot{m}_{in}(h_{in} - h) - \dot{m}_{out}(h_{out} - h) + Q + V\frac{dP}{dt} \tag{2}$$

The input work was calculated by Eq. (3). The motor efficiency and mechanical efficiency obtained from calorimeter tests.

$$W_{comp} = \frac{W_{indi}}{\eta_{motor}\,\eta_{mech}} \tag{3}$$

3.2 Fin-tube type heat exchanger

In this study, the fin-tube type heat exchanger adopted in indoor units. The fin-tube type heat exchanger is modeled by tube-by-tube method. In tube-by-tube method, one tube in a flow path is defined as a control volume. Then heat exchange and pressure drop in a control volume are calculated. And moving boundary method was applied to find a position changing the refrigerant phase. Therefore, the accuracy of prediction on heat exchanger was improved. The heat transfer rate of the fin-tube heat exchanger is calculated by the effectiveness-NTU method as Eq (4).

$$Q = \dot{m}_{air}C_{p,air}\left(T_{air,in} - T_{air,out}\right) = \dot{m}_{ref}(h_{ref,in} - h_{ref,out}) \tag{4}$$

The Correlations of the heat transfer and pressure drop are summarized in Table 2.

Table 2: Correlation of heat transfer and pressure drop coefficient

Fin-tube type heat exchanger	Heat transfer coefficients	**Refrigerant side** -Single phase: Gnielinski -Two Phase: Condensation: Goto Evaporation: Jung-Radermacher **Air side**: Wang
	Pressure drop coefficients	**Refrigerant side** -Single phase: Churchill -Two phase: Condensation: Goto Evaporation: Jung-Radermacher **Air side**: Wang
Plate type heat exchanger	Heat transfer coefficients	**Refrigerant side** -Single phase: kumar -Two phase: Condensation: Han Evaporation: Han **Water side**: Han
	Pressure drop coefficients	**Refrigerant side** -Single phase: kumar -Two phase: Condensation: Han Evaporation: Han

3.3 Plate type heat exchanger

The plate type heat exchanger uses refrigerant and water as working fluids. The model of the plate heat exchanger adopted counter-current flow. In counter-current flow, the working fluids move in opposite directions. The modified effectiveness-NTU method was used to calculate the heat transfer rate of heat exchanger as Eq. (5). The enthalpy of the refrigerant side outlet is calculated as Eq. (6). And The enthalpy of the water is calculated according to Eq. (6).

$$Q = \varepsilon C_{min}\left(T_{ref,in} - T_{water,out}\right)/(1 - \frac{\varepsilon C_{min}}{\dot{m}_{water}, c_{p,water}}) \tag{5}$$

$$h_{ref,out} = h_{ref,in} - \frac{Q}{\dot{m}_{ref}} \tag{6}$$

$$T_{water,in} = T_{water,out} - \frac{Q}{\dot{m}_{water} c_{p,water}} \tag{7}$$

3.4 Electronic expansion valve (EEV)

The mass flow rate of EEVs is calculated by a simple orifice equation as Eq (8).

$$\dot{m}_{EEV} = C_v A \sqrt{\rho_{EEV,in} \Delta P_{EEV}} \tag{8}$$

3.4 Simulation model of the water-cooled VRF system

The operation mode of water-cooled VRF system is divided into cooling-based mode and heating-based mode in this study. The environmental conditions entered the simulation are summarized in Table 3. Figure 2 shows the flow chart of simulation for the water-cooled VRF system with cooling-based mode. The simulation consists of an iterative loop that can satisfy the error of 4 variables. The initial input values for the simulation calculation are the superheat degree of the outdoor unit, the subcooling degree of the indoor unit, and the superheat degree. the mass flow rate and discharge enthalpy calculated through the compressor module. Before calculating the compressor module, condensing pressure, evaporation pressure, suction superheat, MI, HI are assumed. The compressor module calculates the flow rate, enthalpy and input work. The MI and HI parameters are used to calculate the mass flow distributed between the outdoor unit and the indoor unit condenser as Eq (9)-(12). Then, the mass flow rate of the outdoor unit and the indoor unit condenser is calculated.

$$HI_i = HI_{i,n-1} \times \frac{h_{eva,out}}{h_{eve,out,set}} \tag{8}$$

$$MI_i = \frac{HI_i}{HI_{total}} \tag{10}$$

$$\dot{m}_{IDU,i} = \dot{m}_{IDU,total} \times MI_i \tag{11}$$

$$\dot{m}_{ODU} = \dot{m}_{total} - \dot{m}_{IDU,total} \tag{12}$$

The heat transfer rate and pressure drop are calculated in the outdoor unit condenser module to obtain the condenser outlet pressure and enthalpy. Then, the calculated outdoor unit subcooling degree is converged to the input supercooling degree. The pressure drop and heat transfer rate is calculated in the indoor unit condenser module. And

Table 3: The environmental conditions for VRF simulation

Mode		**Indoor**		**Outdoor**
		Air-source		**Water-source**
		Dry bulb temperature (℃)	**Wet bulb temperature (℃)**	**Inlet temperature (℃)**
Cooling based mode	Indoor (heating)	21.1	15.5	30.0
	Indoor (cooling)	27.0	19.0	
Heating based mode	Indoor (heating)	21.1	15.5	20.0
	Indoor (cooling)	27.0	19.0	

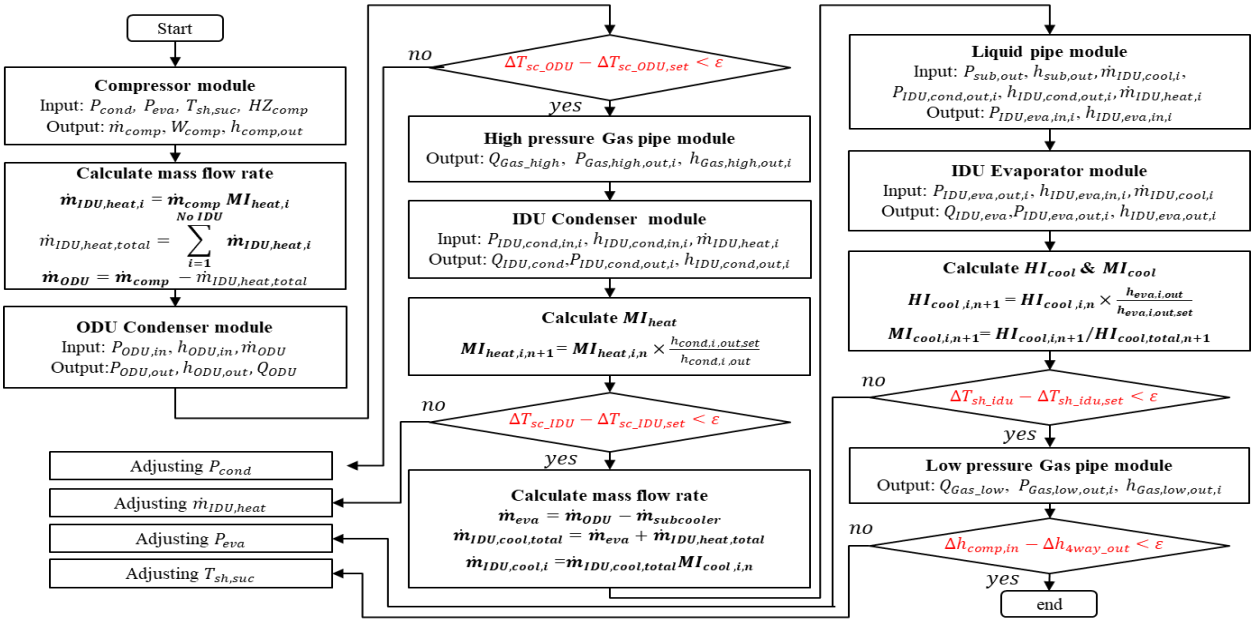

Figure 2: Flow chart for simulation of the water-cooled VRF system with cooling-based mode

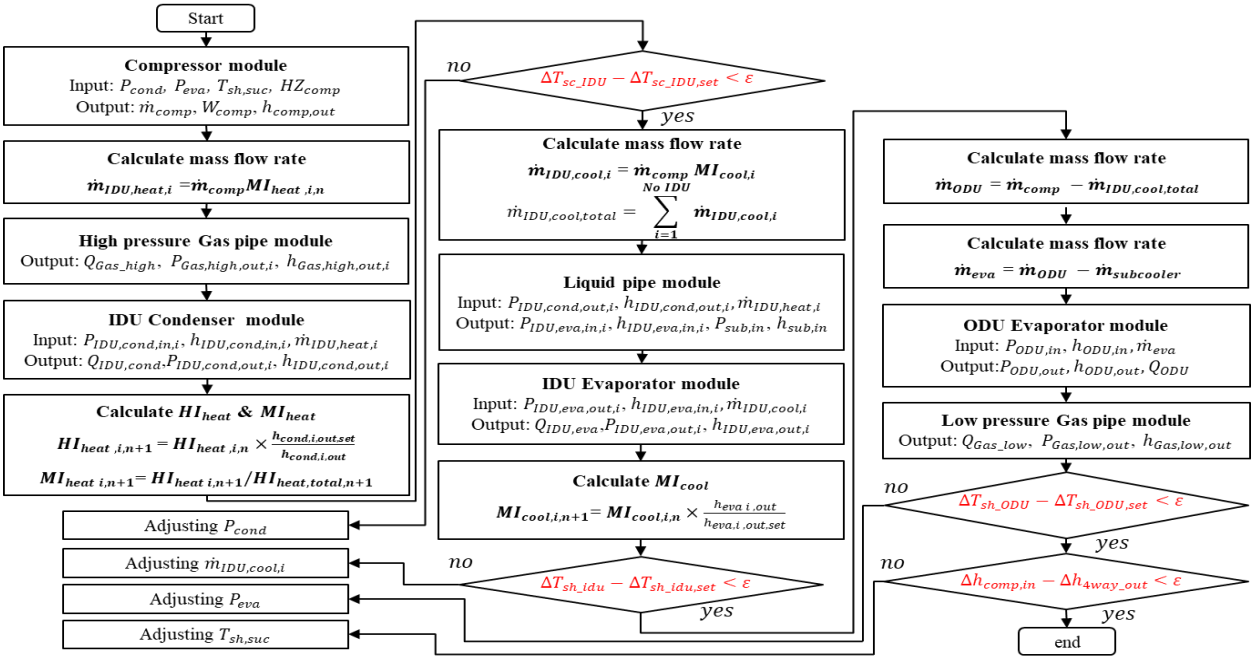

Figure 3: Flow chart for simulation of the water-cooled VRF system with heating-based mode

the MI variable is modified using the condenser outlet data. If the calculated indoor unit subcooling degree does not converge, it is recalculated by returning to the first loop and inputting the corrected MI. before calculating the indoor unit evaporator, the refrigerant of the outdoor unit condenser and the indoor unit condenser are merged. As with the indoor unit condenser, HI and MI are corrected using the calculation result in the indoor unit evaporator module. And it converges the superheat of the indoor unit.

Figure 3 shows the flow chart of simulation for the water-cooled VRF system with heating-based mode. The heating base mode differs from the cooling base mode in the refrigerant flow path. Therefore, the simulation logic is modified. The indoor unit condenser module converges the degree of supercooling of the indoor unit condenser by calculating the pressure drop and heat transfer rate. The refrigerant at the outlet of the indoor unit condenser is distributed from the liquid pipe to the indoor unit evaporator and the outdoor unit evaporator. And the MI is modified to converge the

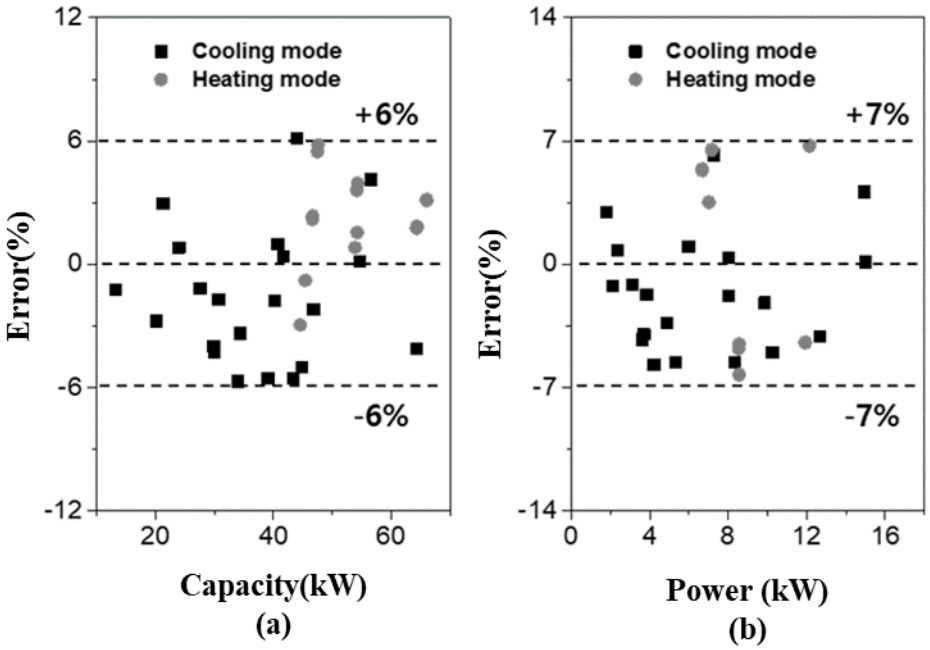

Figure 4: Validation of the simulation (a)capacity and (b) power consumption.

superheat in the indoor unit evaporator module. The outdoor unit evaporator module converges the outdoor unit superheat. The refrigerant is combined with the indoor unit evaporator after the outlet of the outdoor unit evaporator. Then, the simulation ends while converging the compressor suction superheat.

4. VALIDATION

To verify the VRF system simulation, the cooling capacity, heating capacity, and input work of the simulation results were compared with the experimental data according to AHRI standard 1230. Simulation verification was conducted with cooling operation and heating operation. Figure 4. shows the results of verifying the cooling capacity, heating capacity and power consumption measurement. Results from rated and part load capability tests are included. The capacity of cooling and heating contains a maximum error of 6%. The power consumption contains an error of about 6% in cooling mode and 7% in heating mode. The energy performance of the VRF system has less than 10% deviation between simulation and experimental data, so it can be evaluated as reasonable in simulation.

5. RESULTS AND DISCUSSION

The comparison simulation on effects of sub cooling and super heating degree was performed in the water-cooled VRF system. The cooling base model was performed by changing the superheat degree of the indoor unit evaporator to 3 to 9 degrees and increasing the number of indoor unit condensers. Figure 5 and Figure 6 show the condensing pressure and evaporating pressure according to the increase in the number of indoor condensers. As the thermal load of the indoor unit condenser increases, the condensing pressure decreases. And the evaporation pressure increases. In the cooling base mode, the refrigerant after being discharged is distributed between the indoor and outdoor units. Therefore, the refrigerant flow rate distributed to the condenser is reduced, so that the high pressure is lowered. However, the refrigerant from the condenser is combined before the evaporator inlet. As a large amounts of refrigerant flows, the evaporating pressure decreases to meet the superheat in the evaporator. Therefore, the condensing and evaporating pressure of the system is low, and the pressure difference appears to be reduced. Figure 7 shows the total mass flow rate in the VRF system. As the compression ratio decreases, the overall refrigerant flow through the system decreases. As the compression ratio decreases, the total refrigerant flow rate flowing through the system decreases. This effect increases as the number of indoor unit condensers increases. However, as the target superheating degree increases, the flow rate distributed to the indoor unit condenser decreases, so that the effect is reduced. Figure 8 shows the mass flow rate of the indoor unit of condenser.

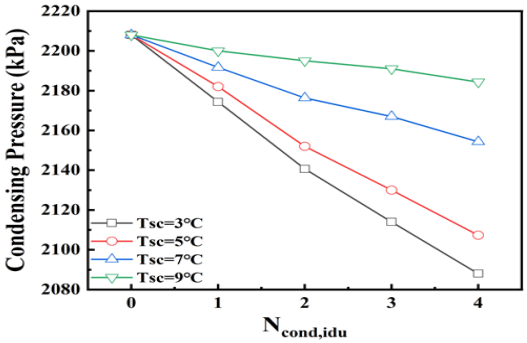

Figure 5: Condensing pressure – cooling based

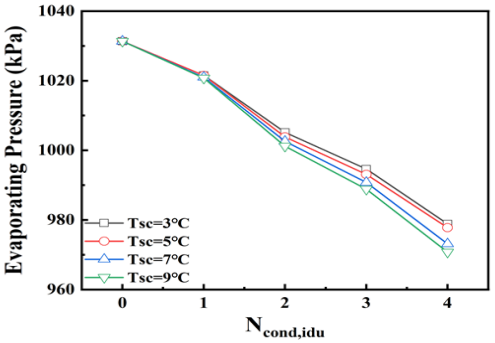

Figure 6: Evaporating Pressure – cooling based

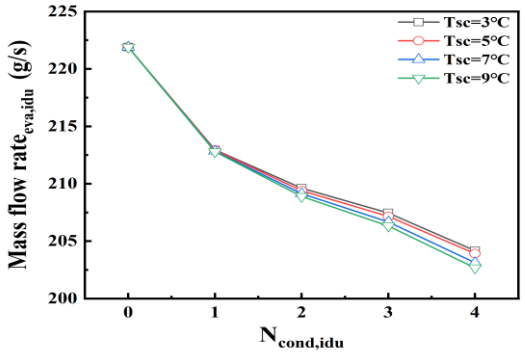

Figure 7: Mass flow rate (Total) – cooling based

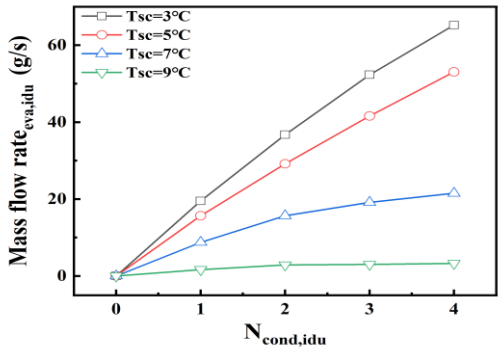

Figure 8: Mass flow rate (IDU. Cond.) – cooling based

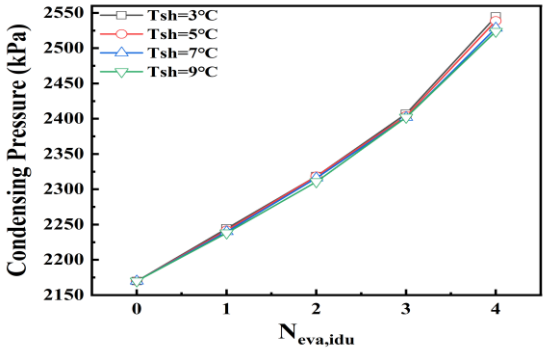

Figure 9: Condensing pressure – heating based

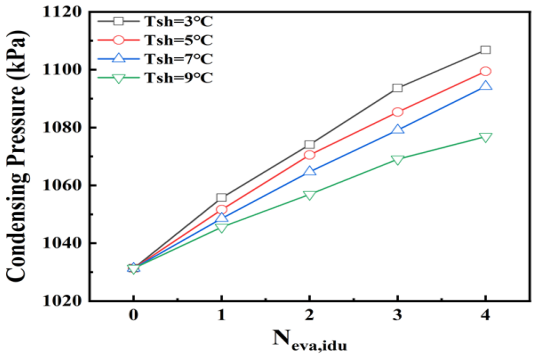

Figure 10: Evaporating Pressure – heating based

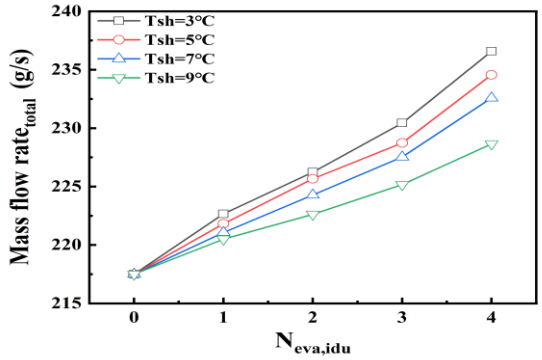

Figure 11: Mass flow rate (Total) – heating based

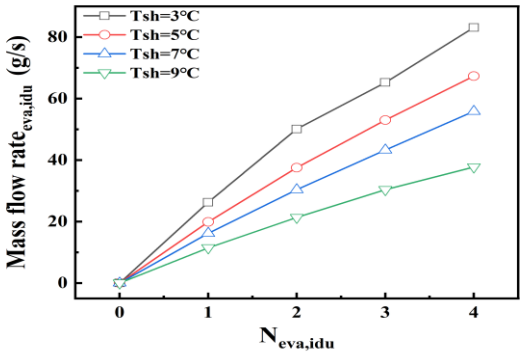

Figure 12: Mass flow rate (IDU. Cond.) – heating based

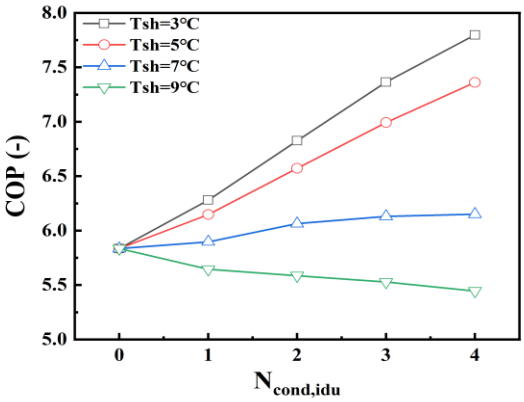

Figure 13: COP – cooling based

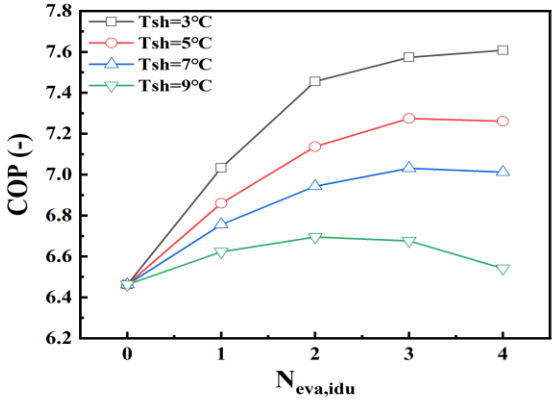

Figure 14: COP – heating based

In the heating-based mode, the trend is opposite to that in the cooling-based mode. Figures 9 and 10 show the condensing pressure and evaporating pressure according to the increase in the number of indoor unit evaporators in the heating-based mode. When the thermal load of the indoor unit evaporator increases, the condensing pressure and the evaporation pressure increase. In the heating-based mode, the refrigerant discharged from the compressor passes through the indoor unit condenser, is separated from the liquid pipe, and is distributed to the indoor unit evaporator and the outdoor unit evaporator. As the number of indoor unit evaporators increases, additional refrigerant is required to satisfy the target superheat degree. As a result, the mass flow through the system increases and the condensing pressure increases. In addition, the refrigerant excluding the refrigerant flowing to the indoor unit from the total mass flow rate flows to the outdoor unit evaporator. Since the total mass flow rate increases as the compression ratio of the system increases, the amount of refrigerant flowing to the outdoor unit evaporator also increases even if the refrigerant is distributed to the indoor unit evaporator. Figure 11 shows the total mass flow rate of the heating-based mode and Figure 12 shows the mass flow rate of the indoor unit of evaporator.

Figures 13 and 14 show the COP of the cooling-based mode and the heating-based mode. In all cases, the COP decreases as the degree of overheating or subcooling of the indoor unit increases. In the cooling-based mode, the COP tends to decrease as the number of indoor unit condensers increases at a high degree of subcooling. However, in the heating-based mode, the COP tends to increase and decrease after a certain section. And the COP reduction is advanced as the superheating degree of the indoor unit evaporator increases.

6. CONCLUSIONS

The effect of the degree of subcooling and superheating of the indoor unit in simultaneous operation of the VRF system was confirmed. In the cooling base mode, as the superheat of the indoor unit condenser increases, the efficiency of the system decreases. And as the number of indoor unit condensers increases, COP increases. However, if the superheating degree of the indoor unit is high, the COP decreases. In the heating base mode, as the degree of supercooling of the indoor unit evaporator increases, the efficiency of the system decreases. And as the number of indoor units increases, COP increases and decreases in a certain section. The performance change of the system was confirmed according to the conditions of the indoor unit. It is judged that the optimization conditions of the cooling base mode and the heating base mode are different. Research is needed to analyze the influence of various parameters such as outdoor units, compressors, and environmental conditions as well as indoor units.

NOMENCLATURE

m	mass	(kg)
h	enthalpy	(kJ/kg)
W	work	(W)
Q	heat transfer rate	(W)
HI	heat indicator	(-)
MI	mass indicator	(-)

Subscript

in	inlet
out	outlet
ind	indicated
sc	subcooling
sh	superheating

REFERENCES

Zhang et al., 2018, A novel Variable Refrigerant Flow (VRF) heat recovery system model: Development and validation., Energy & buildings, Vol. 168, 399-412

Hong et al., 2016, Development and validation of a new VRF model in Energyplus, ASHRAE Winter Conference, OrlandoFLUSA.

Gnielinski et al., 1976, New equations for heat and mass transfer in turbulent pipe and channel flow, Chemical Engineering., Vol.16, 359–369.

Shah, 1979, A general correlation for heat and mass transfer during film condensation inside pipes, Heat Mass Transfer., Vol.22, 547–556.

Kandliker, 1990, A general correlation for saturated two-phase flow boiling heat transfer inside horizontal and vertical tubes, Heat Transfer., Vol.112.

Churchill and Chu, 1977, Friction-factor equation spans all fluid-flow regimes, Adv. Eng. Res., Vol.84, 91–92

Kumar, 1984, The plate heat exchanger: Construction and design, Institute of Chemical Engineering Symposium Series, Vol.86, 1275–1288.

Han, 2003, The characteristics of condensation in brazed plate heat exchangers with different chevron angles, Journal of the Korean Physical Society, Vol.43.

Han, 2003, Experiments on the characteristics of evaporation of R410A in brazed plate heat exchangers with different geometric configurations, Applied Thermal Engineering, Vol.23 ,10

ACKNOWLEDGEMENT

This work was supported by the Human Resources Development program (No. 20204030200030) of the Korea Institute of Energy Technology Evaluation and Planning (KETEP) grant funded by the Korea government Ministry of Trade, Industry and Energy and Korea Institute of Energy Technology Evaluation and Planning(KETEP) grant funded by the Korea government(MOTIE) (20214000000140, Graduate School of Convergence for Clean Energy Integrated Power Generation).